JOURNAL OF AGRICULTURAL AND FOOD CHEMISTRY

Interfacial Interactions of Pectin with Bovine Serum Albumin Studied by Quartz Crystal Microbalance with Dissipation Monitoring: Effect of Ionic Strength

XIAOYONG WANG, CHADA RUENGRUGLIKIT, YU-WEN WANG, AND QINGRONG HUANG*

Department of Food Science, Rutgers University, 65 Dudley Road, New Brunswick, New Jersey 08901, USA

The effect of ionic strength (*I*) on the interfacial interactions between pectin and the bovine serum albumin (BSA) surface has been investigated using the quartz crystal microbalance with dissipation monitoring (QCM-D). As *I* increases from 0.01 to 0.02 M, the frequency shift (ΔF) decreases, whereas the energy dissipation shift (ΔD) changes toward a higher value. Further increase of *I* from 0.02 to 0.5 M causes both ΔF and ΔD to gradually return to almost zero. The adsorbed mass and thickness of the pectin adlayer estimated from the Voigt model confirm that the adsorption of pectin and the formation of thicker pectin adlayers on a BSA surface are favored by the increase of ionic strength at $I = 0.01 \sim 0.02$ M. An increase of *I* above 0.02 M hinders pectin adsorption and causes the formation of a thinner pectin adlayer. The ionic strength-enhanced effect at *I* values lower than 0.02 M is explained as an increase of ionic strength that can screen the electrostatic repulsion to a larger extent than the electrostatic attraction between pectin and BSA. However, when *I* is higher than 0.02 M, both electrostatic repulsion and attraction can be significantly screened by the increasing ionic strength, resulting in the ionic strength-reduced effect. On the other hand, the high viscoelasticity of the pectin adlayer revealed by the Voigt model suggests the formation of a network-structured pectin adlayer on the BSA surface, which contains two steps for higher pectin adsorptions at $I = 0.0125 \sim 0.1$ M by the indication of two slopes in ΔD–ΔF plots.

KEYWORDS: Pectin; bovine serum albumin; interfacial interaction; ionic strength; mass, viscoelastic properties

INTRODUCTION

Interactions between proteins and polysaccharides have attracted increasing interests in the past two decades because of their implications in many biological processes such as the organization of living cell (*1*) and their relevance to many industrial applications, such as microencapsulation (*2*), protein separation and purification (*3*), and processed foods (*4*). The interactions of proteins with polysaccharides in solutions have been extensively investigated and reviewed (*5*–*8*). Protein molecules carrying heterogeneously distributed charges can bind on polysaccharide chains to form soluble protein/polysaccharide complexes at the first critical pH (pH_c), even when protein molecules have the same net charges as polysaccharide chains (*9, 10*). At the second critical pH (pH_φ), which is usually below the protein isoelectric point, strong electrostatic attraction between positively charged protein molecules and anionic polysaccharide chains will cause soluble protein/polysaccharide complexes to aggregate into insoluble protein/polysaccharide complexes, which ultimately settle down to lead to the phase separation. For carboxylic acid–based polysaccharides such as pectin, protein [e.g., bovine serum albumin (BSA)]/polysaccharide (e.g., pectin) insoluble complexes may dissociate into soluble complexes or even uninteracted protein molecules and polysaccharide chains (*11*) with the decrease of pH below its pK_a, because of the low charges of polysaccharide chains as well as the electrostatic repulsion between the positively charged proteins. Because the complex formations between proteins and polysaccharides are mainly driven by the electrostatic interaction, physicochemical parameters, such as pH, ionic strength, polysaccharide linear charge density, protein surface charge density, rigidity of the polysaccharide chain, and protein/polysaccharide ratio, have been demonstrated to strongly influence the protein/polysaccharide interactions in solutions (*5*).

Protein-stabilized emulsions usually are sensitive to environmental stresses such as pH, ionic strength, and temperature, which have limited their applications in many foods (*12*). Recent studies have shown that the resistance of protein-stabilized emulsions to environmental stresses can be improved by adding a polysaccharide that forms protein/polysaccharide complex-

* To whom correspondence should be addressed. E-mail: qhuang@aesop.rutgers.edu, telephone: 732-932-7193, fax: 732-932-6776.

10.1021/jf071714x CCC: $37.00
Published on Web 11/22/2007

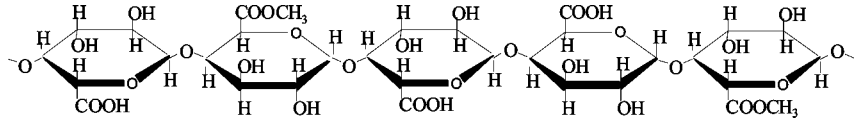

Figure 1. The typical chemical structure of pectin.

based multilayers around oil droplets (*12*). The multilayer emulsions can normally be achieved by mixing a protein-stabilized emulsion and a polysaccharide solution under conditions where there is an attractive force between the polysaccharide molecules and the protein-coated droplet surfaces. However, the addition of polysaccharide may cause bridging flocculation of the protein/polysaccharide complex-based multilayer emulsions *a*. Until now, most of the research on protein/polysaccharide interactions has been limited to bulk solutions. Possibly because of both the complexity of experimental design and the lack of highly sensitive techniques, few works have reported on the interactions of proteins with polysaccharides at the liquid/solid interface, which is very important to the understanding of bridging flocculation that commonly exists in protein/polysaccharide multilayer emulsions (*13a*). Recently, the quartz crystal microbalance (QCM) has obtained much attention outside its traditional development domains of analytical and electroanalytical chemistry (*13*, *14*). On the basis of the piezoelectric effect, QCM is a useful quantitative mass-measuring device at the nanogram level. QCM measures the frequency change (ΔF) of a quartz crystal under the shear oscillation. A new extension of QCM, termed as the quartz crystal microbalance with dissipation monitoring (QCM-D), allows simultaneous time-resolved measurements of the changes in the frequency (ΔF) and the energy dissipation (ΔD) (*15*), which enable QCM-D to provide not only the mass of adlayers, but also the viscoelastic properties of surface-bound molecules. Nowadays, QCM-D has become a popular technique for investigating various biological surface science-related processes, including protein adsorption (*16*, *17*), lipid vesicle adsorption (*18*), bacterial adsorption (*19*), cell adhesion and spreading (*20*), antibody and antigen interaction (*21*), and interactions between peptide and DNA (*22*).

In this paper, QCM-D has been used to study the interactions between pectin and the BSA surface, where BSA is chemically bound on the gold-coated quartz crystal. BSA is a model globular protein with a well-known structure (*23*, *24*). One BSA molecule contains 583 amino acids in a single polypeptide chain with a molecular weight of about 66,000 g/mol. The anionic polysaccharide pectin is a natural polymer extracted from plant cell walls and is used widely not only in the food industry but also in the field of cosmetics and pharmaceutical applications (*25*, *26*). The typical chemical structure of pectin is shown in **Figure 1**. The adsorbed mass, thickness, and viscoelastic properties of the pectin adlayer on the BSA surface in the ionic strength range from 0.01 to 0.5 M have been determined by the combination of QCM-D and the Voigt model.

MATERIALS AND METHODS

Materials. Bovine serum albumin (BSA, ≥98% pure by gel electrophoresis) was purchased from Sigma Chemical Co. and was used without further purification. Low methoxyl pectin with 68% galacturonic residues was kindly provided by Danisco A/S, Denmark and was further purified by dialysis (Spectra/Por dialysis membrane with a molecular weight cutoff equal to 12,000) followed by freeze-drying. The average molecular weight of pectin determined by gel permeation chromatography was approximately 7.0×10^5. 11-Mercaptoundecanoic acid (11-MUA) (Aldrich), N-hydroxysuccinimide (NHS) (Aldrich), 1-ethyl-3-(3-dimethylaminopropyl)carbodiimide hydrochloride (EDC) (Sigma), acetic acid (Aldrich), sodium acetate (Fisher), ammonium hydroxide (NH_4OH) (VWR), hydrogen peroxide (H_2O_2) (Aldrich), sodium chloride (NaCl) (Fisher), and absolute ethanol (Fisher) were all used as received. Milli-Q water was used in all experiments.

Preparation of the BSA Surface. AT-cut quartz crystal coated with gold (fundamental frequency of 5 MHz) was obtained from Q-Sense AB (Sweden). The linkage of BSA onto the gold-coated crystal was carried out using the procedure modified from a previously published paper (*27*). Gold-coated quartz crystal was first cleaned in an UV/ozone chamber for 10 min, followed by immersion in a 1:1:5 mixture of ammonium hydroxide (NH_4OH, 25%), hydrogen peroxide (H_2O_2, 30%), and Milli-Q water for 5 min at 75 °C, and finally, it was placed in an UV/ozone chamber for another 10 min. The gold-coated quartz crystal was then rinsed with Milli-Q water and dried with nitrogen gas (N_2), and the crystal was subsequently soaked in 10 mM 11-MUA solution in absolute ethanol at 60 °C for at least 24 h. The excess amount of 11-MUA was rinsed off with absolute ethanol, and the surface was dried under N_2. Just before the immobilization of protein, the 11-MUA-coated surface was activated by a mixed solution containing 1:1 (v/v) of 100 mg/ml EDC and 100 mg/ml NHS in Milli-Q water for 1 h. A 10 mg/ml BSA solution was used to incubate the active quartz crystal surface at 4 °C for at least 24 h. The BSA chemically linked quartz crystal surface was rinsed out with Milli-Q water and was dried under N_2. The success of functionalization was confirmed by grazing-angle Fourier transform infrared (FTIR) measurements.

Grazing-Angle FTIR. Infrared spectra of BSA-modified quartz crystal surfaces were collected with a FTIR spectrometer (Thermo Nicolet 670, Madison, WI), using the pure gold surface as the background. A Thermo Nicolet Smart Apertured grazing angle (SAGA) accessory with a grazing angle of incidence of 80° was used to collect reflection–absorption infrared spectra. The resolution was set to 4 cm^{-1}, and 1024 scans were collected.

QCM-D Measurements. The interactions between pectin and the BSA chemically linked quartz crystal surface (BSA surface) were studied using a commercial QCM-D apparatus (Q-Sense AB, Sweden) with a Q-Sense D300 electronic unit controlled by computer software (Q-Soft, Q-Sense). A polypropylene pipet tip connecting to the QCM-D chamber was initially filled with pH 4.0 sodium acetate buffer with an appropriate amount of sodium chloride (NaCl) at ionic strengths of 0.01 ~ 0.5 M. By opening the valve, buffer solution was exchanged in the QCM-D chamber via the gravitational flow. After a stable baseline was established, a solution of 0.1 g/L pectin in the same pH 4.0 sodium acetate buffer at the defined ionic strength was exposed to the BSA surface. At the same time, the adsorption was monitored as a function of time by recording the shifts in the frequency (ΔF) and in the energy dissipation (ΔD) simultaneously at the fundamental resonant frequency along with the third, fifth, and seventh overtones until the steady state of the adsorption was reached. The long-term stability of the frequency was within 1 Hz, and this drift was negligible as compared to the frequency shift due to pectin adsorption. All experiments were performed at 25.00 ± 0.02 °C.

RESULTS AND DISCUSSION

Proteins may bind to the self-assembled monolayer of thiol on the gold-coated quartz crystal through either physical adsorption or covalent bonding (*27*, *28*). It was demonstrated that the chemisorbed protein was more stable under physiological conditions because of its much higher bond energy than hydrogen bonding and hydrophobic and electrostatic interactions (*29*). Hence, in the present work, the gold-coated quartz crystals were first treated with an alkanethiol molecule (11-MUA), which could readily form a monolayer and introduce COOH groups

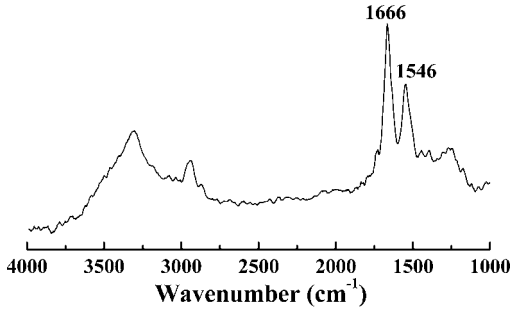

Figure 2. FTIR spectrum of the BSA-modified quartz crystal surface.

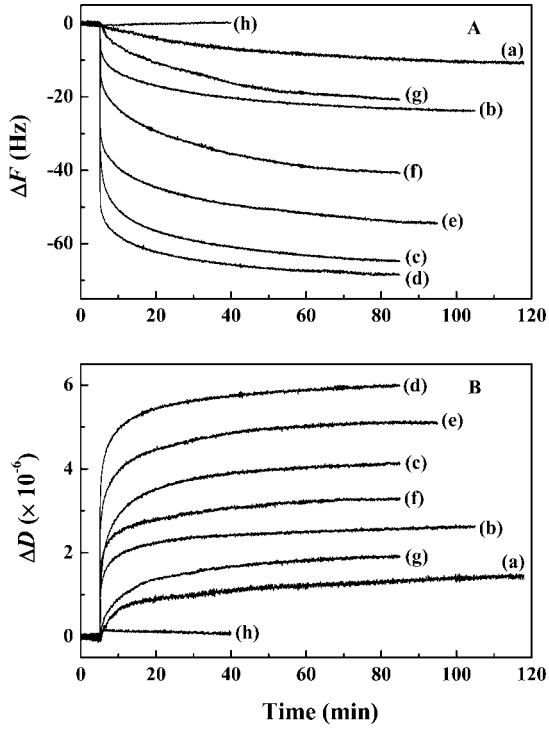

Figure 3. Time-dependent frequency shifts (**A**) and energy dissipation shifts (**B**) for pectin adsorption on the BSA-modified quartz crystal surface at various ionic strengths. (a) $I = 0.01$ M; (b) $I = 0.0125$ M; (c) $I = 0.015$ M; (d) $I = 0.02$ M; (e) $I = 0.06$ M; (f) $I = 0.1$ M; (g) $I = 0.3$ M; (h) $I = 0.5$ M.

to the gold surface (*30*). Then, through the activation of EDC and NHS (*31–33*), BSA could be immobilized on the gold-coated quartz crystal surface through the formation of covalent amide bonds with 11-MUA. As shown in **Figure 2**, the FTIR spectrum of the BSA surface exhibits two characteristic bands of protein amide at 1666 (amide-I) and 1546 cm^{-1} (amide-II), corresponding to the C=O stretch and to the N–H bend coupled with the C–N stretching mode, respectively.

Figure 3 displays the time-resolved resonance frequency shifts (ΔF) and energy dissipation shifts (ΔD) for the third overtone upon the additions of pectin onto the BSA surface at various ionic strengths. Prior to introducing pectin into the chamber, a steady baseline was acquired for about 5 min using pH 4.0 sodium acetate buffer at $I = 0.01$, 0.0125, 0.015, 0.02, 0.06, 0.1, 0.3, and 0.5 M (traces a–h, respectively). As for the ΔF and ΔD curves at $I = 0.01 \sim 0.3$ M, right after each injection of pectin, there was often a rapid decrease in ΔF and a marked increase in ΔD, followed by a much more gradual change of ΔF and ΔD until a steady state was reached. The decreases in ΔF indicates the mass increase of the adsorbed pectin adlayer on the BSA surface, whereas the increases in

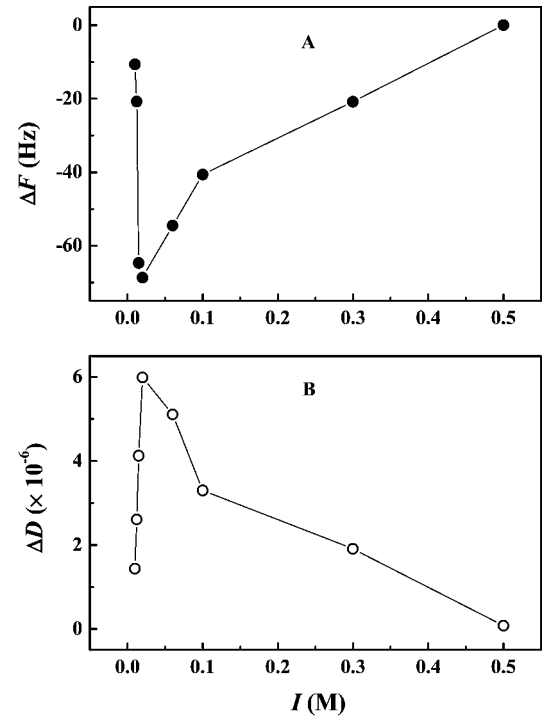

Figure 4. Frequency shifts (**A**) and energy dissipation shifts (**B**) at steady states for pectin adsorption on the BSA-modified quartz crystal surface as a function of ionic strength.

ΔD suggests the formation of viscoelastic pectin adlayers. At $I = 0.5$ M, the values of ΔF and ΔD almost remain constant during the time of investigation, the same as their initial values at the baseline, indicating that there is nearly no pectin adsorption on the BSA surface at such high ionic strength. To clearly see the ionic strength effect on ΔF and ΔD, **Figure 4** gives the variations of ΔF and ΔD at steady state as a function of ionic strength. As I increases from 0.01 to 0.02 M, ΔF decreases, but ΔD changes toward higher values. In contrast, a further increase of I from 0.02 to 0.5 M makes both ΔF and ΔD gradually return to almost zero. Because lower ΔF and higher ΔD values usually indicate stronger adsorption and higher viscoelastic properties of the deposited layer, respectively, the variations of ΔF and ΔD with ionic strength confirms that the increase of I from 0.01 to 0.02 M favors the adsorption of pectin to form more viscoelastic pectin adlayers, but the pectin adsorption is gradually hindered by the further increase of I from 0.02 to 0.5 M, accompanied by forming less viscoelastic pectin adlayers.

Provided that the layer added to the quartz crystal surface is a thin and rigid deposition, the Sauerbrey relationship has been classically employed for the quantitative determination of mass adsorbed on the crystal surface in terms of eq 1, (*34*)

$$\Delta m = -C\Delta F/n \quad (1)$$

where C is the mass sensitivity constant ($C = 17.7$ ng cm^{-2} Hz^{1-} for a 5 MHz crystal), and n is the overtone number ($n = 1, 3, 5, 7...$). According to the Sauerbrey equation, the frequency shift is expected to be proportional to the overtone number. In our work, however, the ratios of the frequency shift with the overtone number ($\Delta F/n$) at different overtones are generally not identical with each other, as shown in the example at $I = 0.01$ M in **Figure 5**. This discrepancy with the Sauerbrey equation is believed to originate from the viscoelastic properties of deposited pectin adlayer on the BSA surface, which is reasonably understood if we consider pectin as a soft material. The

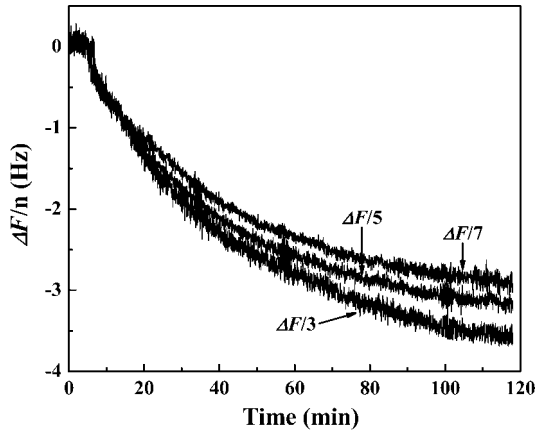

Figure 5. Ratio of the frequency shift with the overtone number as a function of time for pectin adsorption on the BSA-modified quartz crystal surface at $I = 0.01$ M.

Sauerbrey equation is in fact derived from uniform ultrathin rigid films with material properties indistinguishable from those of the quartz crystal (*34*). However, a film that is "soft" (viscoelastic) will not fully couple to the oscillation of the quartz crystal, which dampens the crystal's oscillation and creates additional frequency shifts besides the ones due to the mass load on the electrode surface (*13, 21*). Therefore, the greater extent of pectin adsorption will result in greater invalidation of the Sauerbrey equation, as supported by the differences of $\Delta F/n$ values and the higher ΔD values than $I = 0.01$ M at all other ionic strengths ($I = 0.0125$, 0.015, 0.02, 0.06, 0.1, and 0.3 M; except $I = 0.5$ M, where almost no pectin adsorption).

Taking into account the viscoelastic properties of the system, the Voigt model can allow a more accurate estimation of the mass changes using QCM-D responses (*35*). In this model, ΔF and ΔD of an adsorbed layer can be concisely expressed using eqs 2 and 3,

$$\Delta F \approx -\frac{1}{2\pi\rho_0 h_0}\left\{\frac{\eta_3}{\delta_3} + h_1\rho_1\omega - 2h_1\left(\frac{\eta_3}{\delta_3}\right)^2\frac{\eta_1\omega^2}{\mu_1^2+\omega^2\eta_1^2}\right\} \quad (2)$$

$$\Delta D \approx \frac{1}{\pi f\rho_0 h_0}\left\{\frac{\eta_3}{\delta_3} + 2h_1\left(\frac{\eta_3}{\delta_3}\right)^2\frac{\eta_1\omega^2}{\mu_1^2+\omega^2\eta_1^2}\right\} \quad (3)$$

where ρ_0 and h_0 are the density and thickness of the crystal, respectively, η_3 is the viscosity of the bulk fluid, δ_3 [$= (2\eta_3/\rho_3\omega)$] is the viscous penetration depth of the shear wave in the bulk fluid, ρ_3 is the density of the bulk fluid, and ω is the angular frequency of the oscillation. Here, four unknown parameters of the adsorbed layer, including the thickness, density, viscosity, and elastic shear modulus, are represented by h_1, ρ_1, η_1, and μ_1, respectively. Because the adsorbed layer exhibits different penetration depth of harmonic acoustic frequencies, ΔF and ΔD are measured simultaneously at the fundamental resonant frequency along with the third, fifth, and seventh overtones. As a result, up to eight experimental values of ΔF and ΔD are available (*15*), allowing the model to fit the data and to calculate the mass, thickness, viscosity, and elastic shear modulus of the adsorbed pectin adlayer on the BSA surface.

Figure 6 shows the changes of mass and thickness of the pectin adlayer estimated from the Voigt model at steady state as a function of ionic strength. It is noted that the mass of the

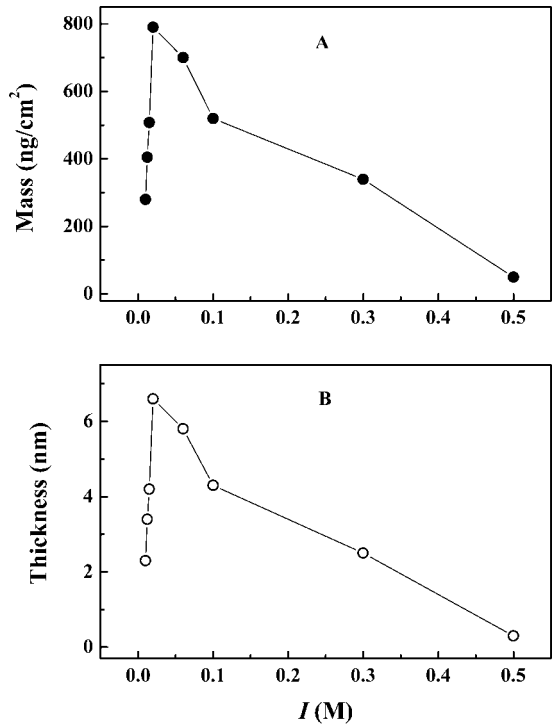

Figure 6. Changes of mass (**A**) and thickness (**B**) of the pectin adlayer for pectin adsorption on the BSA-modified quartz crystal surface as a function of ionic strength estimated from the Voigt model.

pectin adlayer exhibits an increased tendency as I increases from 0.01 to 0.02 M, but a reversed variation is seen when I is further increased from 0.02 to 0.5 M. At pH 4.0, which is lower than the isoelectric point of BSA (pH 4.9), the net charge of BSA molecules is positive, opposite to the negatively charged pectin chains. Hence, the electrostatic interaction of the BSA surface with pectin chains should be the dominant force for pectin adsorption. If the usual ionic strength-reduced interaction due to the salt screening effect is only considered (*5*), then the increase of ionic strength should reduce the electrostatic interaction of BSA with pectin, resulting in a monotonously decreased deposited pectin mass on the BSA surface. However, the increase of the pectin mass at $I = 0.01 \sim 0.02$ M and the reversed case at $I = 0.02 \sim 0.5$ M clearly suggest the enhanced interaction and reduced interaction between pectin and the BSA surface at different ionic strengths, respectively, in agreement with the protein adsorptions of hemoglobin and myoglobin with anionic polysaccharide dextran sulfate in layer-by-layer assembly (*36*). The above interesting ionic strength effect on the interfacial interaction between pectin and the BSA surface is consistent with our previous rheological results of the increasing values of storage modulus (G′) at lower salt concentrations and reversed changes of G′ at higher salt concentrations for β-lactoglobulin/pectin coacervates (*37*), as well as the phase boundary studies of the salt-dependent formation of protein/polysaccharide complexes by other peoples (*38–40*).

The protein molecules are essentially amphoteric polyelectrolytes containing both positive and negative charges. Therefore, there simultaneously exists electrostatic attraction and repulsion between the charges in protein molecules and polysaccharide chains. According to Dubin's model of electrostatic interaction of protein with polyeletrolyte (*39, 41*), the electrostatic attraction and repulsion maybe related to the average distance between the protein's positive sites and the polysaccharide's negative sites (R_+), the average distance between the

protein's negative sites and the polysaccharide's negative sites (R_-), and the Debye length (R_d) by eq 4,

$$U = -\frac{Q_p}{2\epsilon}\left(\frac{Q_+}{R_+}e^{-R_+/R_d} - \frac{Q_-}{R_-}e^{-R_-/R_d}\right) \quad (4)$$

where U is the potential energy for the electrostatic interaction, Q_p is the charge of the segment of the polysaccharide associated with the protein molecule that contains Q_+ positive charges and Q_- negative charges, and ϵ is the dielectric constant. If Q_+, Q_-, R_+, and R_- are independent of ionic strength, then the increase of ionic strength leads to Coulombic screening through influencing R_d [$R_d \approx 0.3/(I^{1/2})$]. During pectin adsorption onto the BSA surface, at lower ionic strengths, there may be $R_+ < R_d < R_-$, and the increase of ionic strength is mainly to screen the electrostatic repulsion but not to disturb the electrostatic attraction between pectin and BSA surface. Consequently, the total interaction will be enhanced with increasing ionic strength. This ionic strength-enhanced effect thus increases pectin mass on the BSA surface when I increases from 0.01 to 0.02 M. On the contrary, when I is above 0.02 M, $R_d < R_+ < R_-$ could make both electrostatic attraction and repulsion be significantly screened because of the higher ionic strength. Therefore, the increase in I beyond 0.02 M leads to a gradual reduced amount of pectin chains adsorbed onto the BSA surface, and there is nearly no pectin adsorption at $I = 0.5$ M.

Another noteworthy observation in **Figure 6** is that the thickness of the pectin adlayer follows the same trend as the mass of the pectin adlayer. The higher the pectin mass, the thicker the pectin adlayer. The variation of the thickness of the pectin adlayer excludes the formation of the pectin monolayer, especially at higher pectin adsorbed mass. One explanation is that when pectin chains adsorb onto the BSA surface at pH 4.0, the BSA positive charges will neutralize the negative charges of the pectin chains. Some electrostatic-neutralized pectin chains bound on the BSA surface at close distances may have somewhat aggregation. Higher pectin adsorption will cause pectin chains to aggregate to a larger extent, which will then contribute to the thickness increase of the pectin adlayer.

The energy dissipation factor (ΔD) measured by QCM-D provides a measure of the rigidity or viscoelasticity of the adsorbed layer. Thin and rigid structures generally have a minimal effect on ΔD, whereas thick and flexible structures may lead to pronounced ΔD. Although it is difficult to directly deduce any information about the adsorbed layer's viscoelasticity by looking at ΔD, the Voigt model could successfully extract quantitative information about the viscoelasticity of the adsorbed layer based on eqs 2 and 3. **Figure 7** shows the variations of viscosity and shear elastic modulus of the pectin adlayer calculated from the Voigt model as a function of ionic strength. Both the viscosity and the shear elastic modulus of the pectin adlayer increase gradually when I increases from 0.01 to 0.02 M, but they decrease to much smaller values when I further increases from 0.02 to 0.5 M, in line with the variation of pectin mass. This observation suggests that the higher pectin adsorption will result in the higher viscosity and shear elastic modulus of the pectin adlayer. In our rheology study (*37*), β-lactoglobulin/pectin coacervates showed remarkable viscoelastic properties, which suggests a highly interconnected gel-like network structure. Although the frequency range for QCM-D is higher than rheology measurements, the viscoelastic behavior of the pectin adlayer given by the Voigt model may also reveal the formation of the network structure of the pectin adlayer on the BSA surface, similar to the previously reported

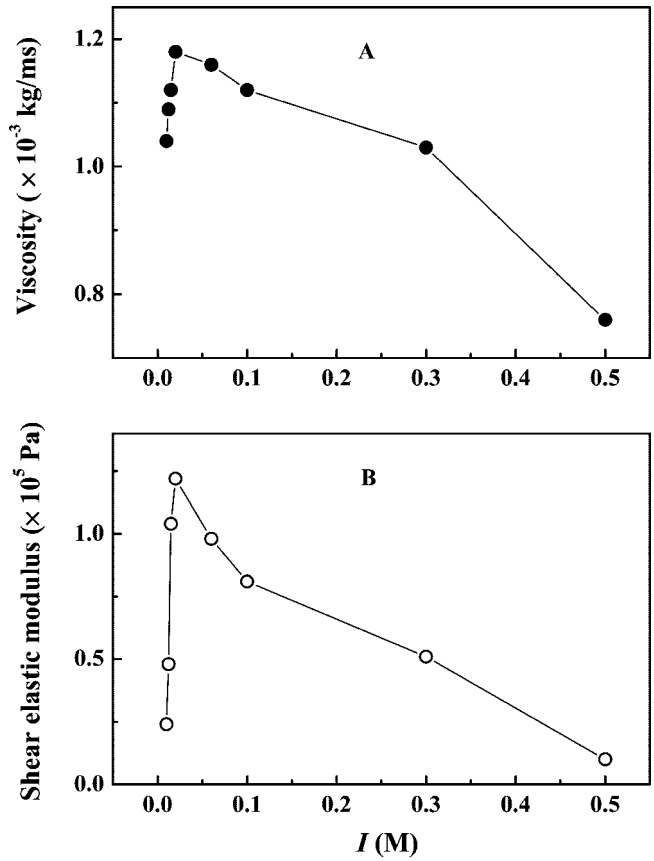

Figure 7. Changes of viscosity (**A**) and shear elastic modulus (**B**) of the pectin adlayer for pectin adsorption on the BSA-modified quartz crystal surface as a function of ionic strength estimated from the Voigt model.

sodium hyaluronate network layer on the BSA surface (*42*). The pectin chain network on the BSA surface may be generated from the aggregation of neutralized pectin chains, which is supported by the previous discussion of the thickness changes of the pectin adlayer. More efficient aggregation of pectin chains resulted from the higher pectin adsorption to give a stronger pectin network structure, leading to higher values of viscosity and shear elastic modulus.

Another way to evaluate the viscoelastic properties of the pectin adlayer is to plot ΔD against ΔF, a so-called ΔD–ΔF plot, from the adsorption kinetics experiments. Using the simultaneously measured ΔF and ΔD in QCM-D responses at the third overtone (**Figure 3**), we have created ΔD–ΔF plots characterizing the viscoelastic nature of the pectin adlayer on the BSA surface at various ionic strengths in **Figure 8**. At the intermediate ionic strengths ($I = 0.0125 \sim 0.1$ M), ΔD–ΔF plots are found to exhibit two slopes. Usually, a smaller slope value of the ΔD–ΔF plot indicates a relatively thinner and more rigid adsorbed layer, whereas a higher slope value signals a thicker and more viscoelastic layer (*43, 44*). Therefore, the ΔD–ΔF plots with two slopes at $I = 0.0125 \sim 0.1$ M indicates that two steps may be involved in the formation of the pectin adlayer with network structure at these ionic strengths. First, the electrostatically adsorbed pectin chains initially form a loosely bound and flexible adlayer, as suggested by the higher first slope than the second slope. Then, the neutralized pectin chains may further aggregate to form a network structure. During the process of pectin chain aggregation, some water molecules coupled with pectin chains may be repelled out, and a more rigid pectin adlayer is finally formed. Compared with the remarkable two-slope ΔD–ΔF plots in $I = 0.0125 \sim 0.1$ M,

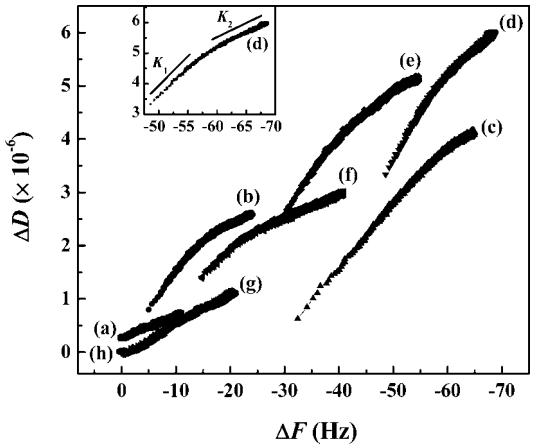

Figure 8. ΔD–ΔF plots at various ionic strengths: (a) $I = 0.01$ M; (b) $I = 0.0125$ M; (c) $I = 0.015$ M; (d) $I = 0.02$ M; (e) $I = 0.06$ M; (f) $I = 0.1$ M; (g) $I = 0.3$ M; (h) $I = 0.5$ M.

Table 1. Slopes of ΔD–ΔF Plots at Various Ionic Strengths

I (M)	0.01	0.0125	0.015	0.02	0.06	0.1	0.3	0.5
K_1 ($\times 10^{-6}$ Hz^{-1})	0.040	0.11	0.12	0.16	0.13	0.096	0.055	0.012
K_2 ($\times 10^{-6}$ Hz^{-1})		0.050	0.063	0.089	0.065	0.044		

which may be attributed to the higher pectin adsorption, the less pectin adsorption should be the reason for the single slope observed in $I = 0.01$, 0.3, and 0.5 M. **Table 1** shows the first slope (K_1) and the second slope (K_2) of ΔD–ΔF plots at various ionic strengths; an example of the determination is shown in the insert of **Figure 8**. The maximum values for K_1 and K_2 at $I = 0.02$ M are consistent with the variations of mass, thickness, and viscoelastic properties of the pectin adlayer determined by the Voigt model. The smaller values of K_2 than K_1 at $I = 0.0125 \sim 0.1$ M suggests that the reorganization of pectin chains on the BSA surface results in denser and more interconnected pectin adlayers.

In conclusion, QCM-D has disclosed two kinds of interfacial interactions between pectin and the BSA surface, including the ionic strength-enhanced effect at $I = 0.01 \sim 0.02$ M, and the ionic strength-reduced effect at $I = 0.02 \sim 0.5$ M. The adsorbed mass, thickness, viscosity, and shear elastic modulus of the pectin adlayer calculated from the Voigt model suggest the high viscoelasticity and the network structure of the pectin adlayer. In the future, it is valuable to use QCM-D combined with other state-of-the-art methodologies such as AFM and surface plasmon resonance to continuously investigate the influences of other electrostatic factors including pH, polysaccharide linear charge density, protein surface charge density, and rigidity of the polysaccharide chain on the protein/polysaccharide interfacial interactions. Our research is expected to facilitate the understanding of the mechanism that leads to the formation of stable polysaccharide/protein complex-based multilayer food emulsions.

LITERATURE CITED

(1) Berdick, M.; Morawetz, H. The interaction of catalase with synthetic polyelectrolytes. *J. Biol. Chem.* **1954**, *206*, 959–971.

(2) Burgess, D. J.; Carless, J. E. Microelectrophoretic studies of gelatin and acacia for the prediction of complex coacervation. *J. Colloid Interface Sci.* **1984**, *98*, 1–8.

(3) Dubin, P. L.; Gao, J.; Mattison, K. W. Protein purification by selective phase separation with polyelectrolytes. *Sep. Purif. Methods* **1994**, *23*, 1–16.

(4) Tolstoguzov, V. B. Functional properties of food proteins and role of protein–polysaccharide interaction. *Food Hydrocoll.* **1991**, *4*, 429–468.

(5) Schmitt, C.; Sanchez, C.; Desobry-banon, S.; Hardy, J. Structure and technofunctional properties of protein–polysaccharide complexes: a review. *Crit. Rev. Food Sci. Nutr.* **1998**, *38*, 689–753.

(6) Doublier, J.-L.; Garnier, C.; Renard, D.; Sanchez, C. Protein–polysaccharide interactions. *Curr. Opin. Colloid Interface Sci.* **2000**, *5*, 202–214.

(7) Turgeon, S. L.; Beaulieu, M.; Schmitt, C.; Sanchez, C. Protein–polysaccharide interactions: phase-ordering kinetics, thermodynamic and structural aspects. *Curr. Opin. Colloid Interface Sci.* **2003**, *8*, 401–414.

(8) de Kruif, C. G.; Weinbreck, F.; de Vries, R. Complex coacervation of proteins and anionic polysaccharides. *Curr. Opin. Colloid Interface Sci.* **2004**, *9*, 340–349.

(9) Park, J. M.; Muhoberac, B. B.; Dubin, P. L.; Xia, J. Effects of protein charge heterogeneity in protein–polyelectrolyte complexation. *Macromolecules* **1992**, *25*, 290–295.

(10) Xia, J.; Dubin, P. L. Protein–polyelectrolyte complexes. In *Macromolecular Complexes in Chemistry and Biology*, Dubin, P. L.; Bock, J.; Davis, R. M.; Schulz, D. N.; Thies, C., Eds.; Springer-Verlag: Berlin, 1994; pp 247–271.

(11) Dickinson, E. Stability and rheological implications of electrostatic milk protein-polysaccharide interactions. *Trends Food Sci. Technol.* **1998**, *9*, 347–354.

(12) McClements, D. J. *Food Emulsions: Principles, Practices, and Techniques*, 2nd ed., CRC Press, Boca Raton, Florida; 2004.

(13) (a) McClements, D. J. Theoretical analysis of factors affecting the formation and stability of multilayered colloidal dispersions. *Langmuir* **2005**, *21*, 97779785. (b) Ward, M. D. Principles and applications of the electrochemical quartz crystal microbalance. In *Physical Electrochemistry: Principles, Methods & Applications*; Rubenstein, I., Ed.; Marcel Dekker: New York, 1995; pp 293–338. (c) Janshoff, A.; Galla, H. J.; Steinem, C. Piezoelectric mass-sensing devices as biosensors—an alternative to optical biosensors. *Angew. Chem., Int. Ed.* **2000**, *39*, 40044032.

(14) Marx, K. A. Quartz crystal microbalance: A useful tool for studying thin polymer films and complex biomolecular systems at the solution-surface interface. *Biomacromolecules* **2003**, *4*, 1099–1120.

(15) Weber, N.; Wendel, H. P.; Kohn, J. Formation of viscoelastic protein layers on polymeric surfaces relevant to platelet adhesion. *J. Biomed. Mater. Res. A* **2005**, *72*, 420–427.

(16) Höök, F.; Kasemo, B.; Nylander, T.; Fant, C.; Sott, K.; Elwing, H. Variations in coupled water, viscoelastic properties, and film thickness of a mefp-1 protein film during adsorption and cross-linking: a quartz crystal microbalance with dissipation monitoring, ellipsometry, and surface plasmon resonance study. *Anal. Chem.* **2001**, *73*, 5796–5804.

(17) Höök, F.; Voros, J.; Rodahl, M.; Kurrat, R.; Boni, P.; Ramsden, J. J.; Textor, M.; Spencer, N. D.; Tengvall, P.; Gold, J.; Kasemo, B. A comparative study of protein adsorption on titanium oxide surfaces using in situ ellipsometry, optical waveguide lightmode spectroscopy, and quartz crystal microbalance/dissipation. *Colloids Surf., B* **2002**, *24*, 155–170.

(18) Keller, C. A.; Kasemo, B. Surface specific kinetics of lipid vesicle adsorption measured with a quartz crystal microbalance. *Biophys. J.* **1998**, *75*, 1397–1402.

(19) Fredriksson, C.; Khilman, S.; Kasemo, B.; Steel, D. M. In vitro real-time characterization of cell attachment and spreading. *J. Mater.Sci.: Mater. Med.* **1998**, *9*, 785–788.

(20) Fredriksson, C.; Kihlman, S.; Rodahl, M.; Kasemo, B. The piezoelectric quartz crystal mass and dissipation sensor: a means of studying cell adhesion. *Langmuir* **1998**, *14*, 248–251.

(21) Höök, F.; Rodahl, M.; Brzezinski, P.; Kasemo, B. Energy dissipation kinetics for protein and antibody-antigen adsorption under shear oscillation on a quartz crystal microbalance. *Langmuir* **1998**, *14*, 729–734.

(22) Höök, F.; Ray, A.; Norden, B.; Kasemo, B. Characterization of PNA and DNA immobilization and subsequent hybridization with DNA using acoustic-shear-wave attenuation measurements. *Langmuir* **2001**, *17*, 8305–8312.
(23) Foster, J. F. Some aspects of the structure and conformational properties of serum albumin. In *Albumin Structure, Function and Uses*; Rosenoer, V. M., Oratz, M., Rothschild, M. A., Eds.; Pergamon Press: Oxford, United Kingdom, 1977; pp 53–84.
(24) Peters, T. J. All about Albumin Biochemistry, Genetics, and Medical Applications; Academic Press; San Diego, California, 1996.
(25) Oakenfull, D. G. The chemistry of high-methoxy pectins. In *The Chemistry and Technology of Pectin*; Walter, R. H. Eds.; Academic Press: New York, 1991; pp 88–108.
(26) Thakur, B. R.; Singh, R. K.; Handa, A. K. Chemistry and uses of pectin—a review. *Crit. Rev. Food Sci. Nutr.* **1997**, *37*, 47–73.
(27) Patel, N.; Davies, M. C.; Heaton, R. J.; Roberts, C. J.; Tendler, S. J. B.; Williams, P. A scanning probe microscopy study of the physisorption and chemisorption of protein molecules onto carboxylate terminated self-assembled monolayers. *Appl. Phys. A: Mater. Sci. Process.* **1998**, *66*, S569–S574.
(28) Si, S.; Si, L.; Ren, F.; Zhu, D.; Fung, Y. Study of adsorption behavior of bilirubin on human-albumin monolayer using a quartz crystal microbalance. *J. Colloid Interface Sci.* **2002**, *253*, 47–52.
(29) Nakata, S.; Kido, N.; Hayashi, M.; Hara, M; Sasabe, H.; Sugawara, T.; Matsuda, T. Chemisorption of proteins and their thiol derivatives onto gold surfaces: characterization based on electrochemical nonlinearity. *Biophys. Chem.* **1996**, *62*, 63–72.
(30) Su, X.; Zhang, J. Comparison of surface plasmon resonance spectroscopy and quartz crystal microbalance for human IgE quantification. *Sens. Actuators B* **2004**, *100*, 309–314.
(31) Frey, B. L.; Corn, R. M. Covalent attachment and derivatization of poly(L-lysine) monolayers on gold surfaces as characterized by polarization-modulation FT-IR spectroscopy. *Anal. Chem.* **1996**, *68*, 3187–3193.
(32) Liu, Y. C.; Wang, C. M.; Hsiung, K. P. Comparison of different protein immobilization methods on quartz crystal microbalance surface in flow injection immunoassay. *Anal. Biochem.* **2001**, *299*, 130–135.
(33) Kim, J.; Yamasaki, R.; Park, J.; Jung, H.; Lee, H.; Kawai, T. Highly dense protein layers confirmed by atomic force microscopy and quartz crystal microbalance. *J. Biosci. Bioeng.* **2004**, *97*, 138–140.
(34) Sauerbrey, G. Verwendung von schwingquarzen zur wägung dünner schichten und zur mikrowägung (The use of quartz oscillators for weighing thin layers and for microweighing). *ZPhys-e.A: Hadrons Nucl.* **1959**, *155*, 206–222.
(35) Voinova, M. V.; Rodahl, M.; Jonson, M.; Kasemo, B. Viscoelastic acoustic response of layered polymer films at fluid-solid interfaces: continuum mechanics approach. *Phys. Scr.* **1999**, *59*, 391–396.
(36) He, P.; Hu, N. Interactions between heme proteins and dextran sulfate in layer-by-layer assembly films. *J. Phys. Chem. B* **2004**, *108*, 13144–13152.
(37) Wang, X.; Lee, J.; Wang, Y.; Huang, Q. Composition and rheological properties of β-lactoglobulin/pectin coacervates: effects of added salt and initial protein/polysaccharide ratio. *Biomacromolecules* **2007**, *8*, 992–997.
(38) Weinbreck, F.; de Vries, R.; Schrooyen, P.; de Kruif, C. G. Complex coacervation of whey proteins and gum arabic. *Biomacromolecules* **2003**, *4*, 293–303.
(39) Seyrek, E.; Dubin, P. L.; Tribet, C.; Gamble, E. A. Ionic strength dependence of protein-polyelectrolyte interactions. *Biomacromolecules* **2003**, *4*, 273–282.
(40) Weinbreck, F.; Nisuwenhuijse, H.; Robijn, G. W.; de Kruif, C. G. Complexation of whey proteins with carrageenan. *J. Agric. Food Chem.* **2004**, *52*, 3550–3555.
(41) Hattori, T.; Hallberg, R.; Dubin, P. L. Roles of electrostatic interaction and polymer structure in the binding of β-lactoglobulin to anionic polyelectrolytes: measurement of binding constants by frontal analysis continuous capillary electrophoresis. *Langmuir* **2000**, *16*, 9738–9743.
(42) Nonogaki, T.; Xu, S.; Kugimiya, S.; Sato, S.; Miyata, I.; Yonese, M. Two dimensional auto-organized nanostructure formation of hyaluronate on bovine serum albumin monolayer and its surface tension. *Langmuir* **2000**, *16*, 4272–4278.
(43) Rodahl, M.; Höök, F.; Fredriksson, C.; Keller, C. A.; Krozer, A.; Brzezinski, P.; Voinova, M.; Kasemo, B. Simultaneous frequency and dissipation factor QCM measurements of biomolecular adsorption and cell adhesion. *Faraday Discuss.* **1997**, *107*, 229–246.
(44) Zhou, C.; Friedt, J.-M.; Angelova, A.; Choi, K.-H.; Laureyn, W.; Frederix, F.; Francis, L. A.; Campitelli, A.; Engelborghs, Y.; Borghs, G. Human immunoglobulin adsorption investigated by means of quartz crystal microbalance dissipation, atomic force microscopy, surface acoustic wave, and surface plasmon resonance techniques. *Langmuir* **2004**, *20*, 5870–5878.

Received for review June 11, 2007. Revised manuscript received September 25, 2007. Accepted October 4, 2007. This project is supported by the Center for Advanced Food Technology (CAFT), and in part by the United States Department of Agriculture National Research Initiative (USDA-NRI).

JF071714X